JOURNAL OF GEOPHYSICAL RESEARCH, VOL. 106, NO. D3, PAGES 2963–2973, FEBRUARY 16, 2001

UV-B optical thickness observations of the atmosphere

V. W. J. H. Kirchhoff,[1] A. A. Silva,[2] C. A. Costa,[3] N. Paes Leme,[1]
H. G. Pavão,[4] F. Zaratti[5]

Abstract. The optical thickness of the atmosphere, τ, was deduced from measurements of narrowband direct solar UV-B radiation. A measurement campaign was organized to obtain the radiation at three different sites, during the month of August 1999, using the same methods and instruments, in order to deduce the atmospheric optical thickness in the spectral UV-B range (280-320 nm). The three observation sites were chosen to cover a wide range of measurement conditions; located near the tropical Atlantic Ocean (Natal, 5.8°S, 35.2°W), on the Andes mountains (La Paz, 16.5°S, 68.1°W), and in the biomass burning area of central Brazil (Campo Grande, 19.2°S, 54.3°W). The UV-B measurements were made with a Brewer spectrophotometer at each site. Since the instrument measures atmospheric ozone and SO_2 simultaneously, it is possible, from the total atmospheric optical thickness τ, to deduce the aerosol optical thickness $\tau_{aerosol}$. The results have been combined in different ways to compare with satellite data, showing good performance. Time variations as short as about 10 min can be seen. On clear days the time variations are relatively small, as expected. On the other hand, for the biomass burning site, for conditions of mixed air masses (the instrument is not looking directly at plumes) one can see very large variations in τ in relatively short time intervals, for example, for one case, from 3.5 to 7.0 in about 30 min. Absolute values for τ at Natal and La Paz were near 2.0 and at Campo Grande, between 2.5 and 3.0, but with occasional highs of about 4.5. For $\tau_{aerosol}$, Natal and La Paz had values between 0.0 and 0.4, whereas Campo Grande had most values near 0.4, with occasional highs near 1.0, 1.2, and 2.2.

1. Introduction

The portion of the solar radiation spectrum, object of this study, is known as UV-B, or biologically active solar radiation [*Frederick and Lubin*, 1988]. The objective of the experiment was to optimize the acquisition of direct solar UV-B radiation data (see wavelengths in Table 1), in order to deduce the optical thickness (τ) of the atmosphere by the Langley method [*Qiu*, 1998; *Kyllen et al.*, 1998; *Wenny et al.*, 1998]. The experiment was designed to obtain data at regular intervals (in terms of the cosine of the solar zenith angle). Several time intervals to obtain τ were experimented in order to evaluate its variability as a function of time, but usually obtaining average values during morning and afternoon hours was preferred.

The Campo Grande site was especially set up for this experiment. A Brewer spectrophotometer, normally sited at the Instituto Nacional de Pesquisas Espaciais (INPE) headquarters in Sao Jose dos Campos, Sao Paulo, was taken to Campo Grande and operated during approximately 1 month at the Empresa de Pesquisa, Assistência Técnica e Extensão Rural (EMPAER) facility, outside of the urban perimeter of the city. This site is located within a savanna environment, locally known as cerrado. In this vast region of nearly 3 million km^2, biomass burning is a seasonal, recurrent event [*Kirchhoff*, 1996]. Randomly located large areas can be set afire in this region. During these episodes large amounts of soot carbon, particles, and carbon monoxide are injected into the atmosphere. In general, ozone is then produced in the lower atmosphere [*Olson et al.*, 1996; *Longo et al.*, 1999]. In the visible region of the spectrum, optical thicknesses of the atmosphere were obtained by *Ross et al.*, [1997], for example, and *Krishnamurti et al.*, [1998] have investigated the transport and influence of aerosols over pristine regions and their influence on radiative forcing. The objective of the experiment in Campo Grande was to determine, for the first time, the UV-B optical thickness of the atmosphere, and its variation with time during biomass burning. With additional observations made at two other sites with very different characteristics, the absolute values of τ have been compared.

1.1. Instruments

The Brewer spectrophotometer is a commercial instrument in wide use globally that was originally designed to measure the total column of ozone in the atmosphere [*Brewer*, 1973]. For the spectral separation of the solar radiation it uses an Ebert type spectrometer, with an effective F6 optical aperture, and a diffraction grating of 1200 lines mm^{-1}. The UV-B wavelengths in the Brewer ozone mode are separated in five channels, shown in

[1] Instituto Nacional de Pesquisas Espaciais, São José dos Campos, São Paulo, Brazil
[2] Pontifícia Universidade Católica de Minas Gerais, Belo Horizonte, Minas Gerais, Brazil
[3] Empresa de Pesquisa, Assistência Técnica e Extensão Rural, Campo Grande, Mato Grosso, Brazil
[4] Fundação Universidade Federal de Mato Grosso do Sul, Campo Grande, Mato Grosso, Brazil
[5] Universidad Mayor de San Andres, UMSA, La Paz, Bolivia

Copyright 2001 by the American Geophysical Union.

Paper number 2000JD900506.
0148-0227/01/2000JD900506$09.00

Table 1. Nominal Brewer UV-B Wavelengths Used for Ozone Measurements

Channel	Wavelength, nm
1	306.3
2	310.1
3	313.5
4	316.8
5	320.1

Table 1. In addition to ozone, the more recent instruments allow also the observation of NO_2, SO_2, and global UV-B radiation. The Canadian built Brewer spectrophotometer is totally automatic and can be programmed to perform the observations as necessary for each special interest. In Brazil, this instrument has been used to observe stratospheric ozone and UV-B variations [*Kirchhoff et al.*, 1997a], the ozone hole in the Antarctic region [*Kirchhoff et al.*,1997b; 1997c] and atmospheric SO_2 of volcanic origin [*Sahai et al.*, 1997]. *Fioletov et al.* [1998] have used a similar instrument for measurements in Europe. In the present case, the instruments were programmed to perform direct Sun observations at regular intervals of the solar zenith angle at each of the three stations. The instruments measured direct solar count rates during observation periods of about 90 min, in the morning and afternoon with solar zenith angles less than 60°.

1.2. Sites and Methods

Biomass burning values of τ were obtained by specially setting up a Brewer spectrophotometer in the dry cerrado region of Campo Grande, Brazil (see coordinates in Table 2). In addition to Campo Grande, 2 other sites were operated simultaneously. These used the same instruments and methods to obtain τ. Natal, Brazil, is a permanent observation site near the Atlantic coast of northeast Brazil. This site is used regularly to make ozonesonde observations of the vertical distribution of ozone in the troposphere and stratosphere; it is a site near the shoreline, and always receives air masses from the Atlantic Ocean. The air masses are thus not influenced by the nearby city, but as discussed by *Logan and Kirchhoff* [1986], the atmosphere of Natal may have a secondary, minor influence from far away biomass burning practices (from Brazil and Africa). Burning products may be transported by a combination of vertical dry (and wet) convection and stratospheric (or tropospheric for the case of the African contribution) horizontal transport toward Natal. A third site operates on the Andes mountains, at La Paz, Bolivia, altitude 3420 m, also a permanent observation site operated by INPE and the Universidad Mayor de San Andres.

The optical thickness is deduced from the UV-B direct solar radiation at each wavelength by using the Langley method. This method is based on Beer's law,

$$I_\lambda = I_{o\lambda} \exp(-\tau m)$$

where I_λ is the measured radiation intensity at wavelength λ, at ground level, after being attenuated by the medium of extinction coefficient τ; $I_{o\lambda}$ is the intensity before entering the medium, that is, at the top of the atmosphere, and m is the air mass (in the most simple case equal to the secant of the solar zenith angle). In the Langley method the natural logarithm is applied to the radiation values, which are plotted as a function of the air mass. The inclination of the resulting straight line is τ, the total optical thickness (or optical depth) at a given wavelength (note therefore that τ does not depend on the absolute intensity of the radiation).

The major requirements/assumptions for the applicability of the Langley method can be summarized as follows: (1) direct solar radiation; (2) monocromatic radiation; (3) the extraterrestrial radiation at the top of the atmosphere is constant during the time interval considered for the application of the method; (4) the optical thickness of the atmosphere is constant during the time interval considered for the application of the method. These requirements have been easily satisfied with the Brewer spectrophotometer data.

The total atmospheric optical thickness can be written as

$$\tau = \tau_{ozone} + \tau_{aerosol} + \tau_{Rayleigh} + \tau_{SO2}$$

the summation of four main components, one for ozone (τ_{ozone}), one for aerosol ($\tau_{aerosol}$), one for Rayleigh contributions ($\tau_{Rayleigh}$), and one for the contribution of absorption by SO_2 (τ_{SO2}). The great advantage of the Brewer observations is that it measures also the ozone and SO_2 columns. Since the Rayleigh contribution can be easily calculated [*Froehlich and Shaw*, 1980; *Teillet*, 1990], it is possible by this method to isolate the optical thickness of the aerosol contribution, $\tau_{aerosol}$. The numerical values, the time variations in the biomass burning region, as well as the results at a pristine site and a mountain site will be described.

2. Results and Discussion

2.1. The Dry Regions in Brazil

The severest dry regions in Brazil, where the fires are more frequent, are shown in Plate 1. In this plate, using August 30, 1999, as a reference, the numbers of previous days without any rain are shown. For the region in central Brazil (darkest area, in brown), no rains have occurred for more than 60 days. This is the cerrado region where most of the fires detected by satellites are seen. According to Plate 1, Campo Grande is located in an area where no rains were seen for more than 60 days. Clearly, this situation makes the local vegetation very dry and prone to catch fire. In contrast, at Natal, the last rain occurred only 0-1 days before (August 30), a situation that is common for most of the seashore sites.

Similar to the lack of precipitation map shown in Plate 1, the distribution of relative humidity over the states of Brazil is such that the dryest area is seen covering the states of Mato Grosso and Mato Grosso do Sul (capital, Campo Grande). From about the equator downward to 30° the humidity is between 25 and 50%, with only very small patches of higher values. A majority of fires generally occurs in the north of the state of Mato Grosso, between about 9° and 12°S, along the meridian of 55°W, and in the south and east of the state of Para, between about 5° and 10°S, near the

Table 2. Observation Sites: Natal (Brazil), La Paz (Bolivia), and Campo Grande (Brazil)

Site Name	Latitude, °S	Longitude, °W	Altitude, m
Natal	5.84	35.21	30
La Paz	16.54	68.06	3.420
Campo Grande	19.25	54.34	600

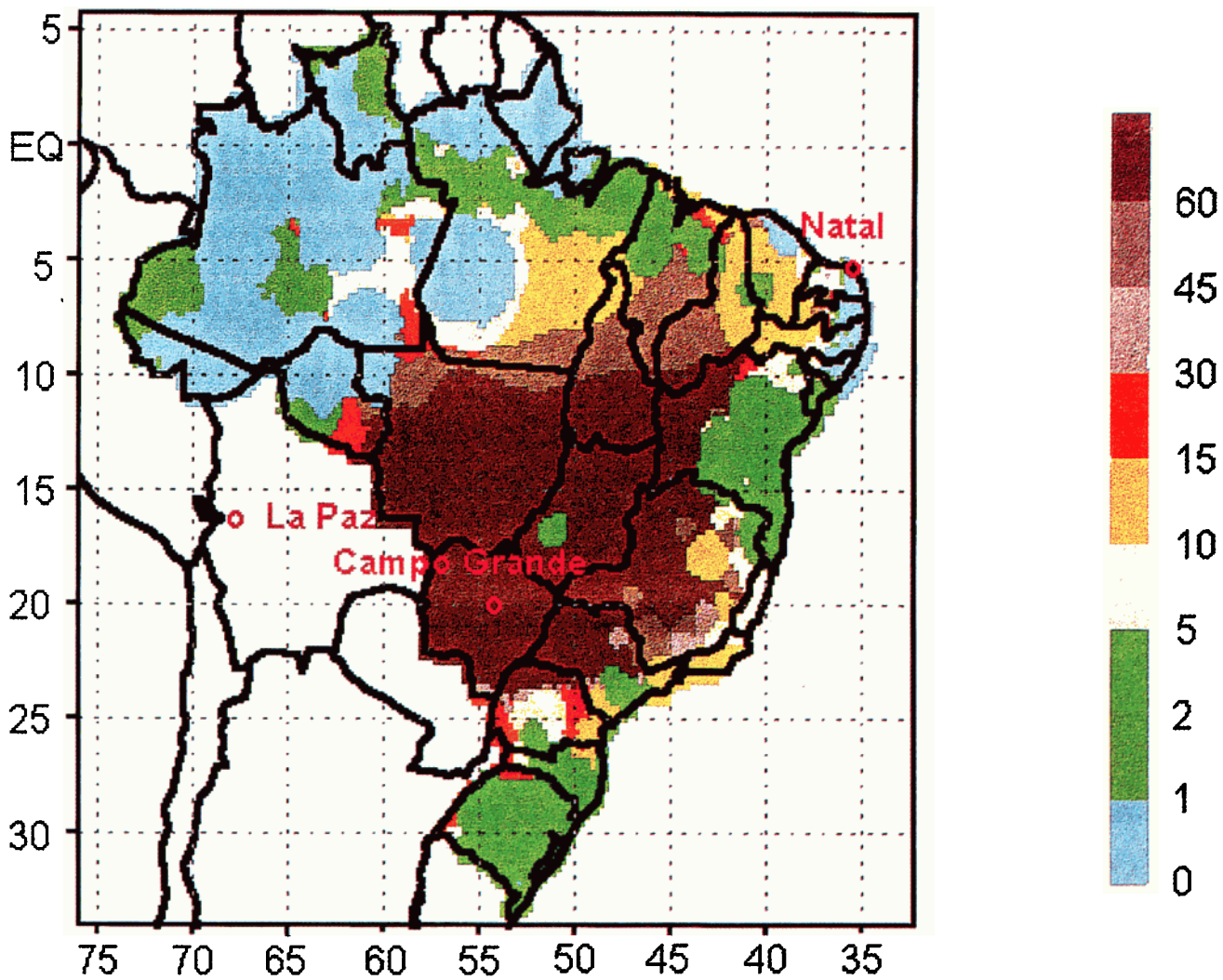

Plate 1. Map of Brazil, divided in states, showing the number of days with no precipitation before August 30, in color codes. It shows wet regions in Amazonia and on the Atlantic shoreline, and a very dry region in central Brazil, the so-called cerrado region (dark brown). The color codes start from light blue (up to 1 day), and go to dark brown (more than 60 days without rain).

meridian of 50°W. This region represents the transition between the cerrado and forest environments.

2.2. UV-B Observations

A typical diurnal variation of the direct solar radiation measured by the Brewer spectrophotometer at 306.3 nm is shown in Figure 1, for La Paz, Bolivia, on September 3, 1997. The Langley plot corresponding to this UV-B data is shown in Figure 2, for the morning period, representing a sequence of observations in a relatively homogeneous and clean atmosphere, in space and time. Note that the small irregularities seen in Figure 1 near noon are not a problem in the Langley plot. The solar zenith angle span corresponds to approximately 24° to 55°.

There is an excellent fit of the data points to the Langley straight line (R^2=0.99). The total optical thickness in this case is τ=1.78. The actual data points are shown, and the linear fit. It took about 3 min to obtain one direct Sun UV-B data set with all the wavelengths shown in Table 1, or roughly, a measurement period with some 19-20 observations took about 1.5 hours. In general, measurement periods of 1.5 hours were held in the morning and in the afternoon periods.

Measurements are made in a rather well mixed atmosphere, not entirely homogeneous, but also not individual plume cases; it is thought that this is representative of the general smoke cover in the area during biomass burning. Note that only a clear atmosphere responds strictly to the Langley method requirements, namely, that τ should remain constant during the observation period. The situation is more complicated in the biomass burning region, with smoke cover, which is almost never quite homogeneous. This is caused by the heterogeneous and random distribution of the sources, in space and time, the mixing conditions in the atmosphere, and wind direction and velocity. It is assumed, therefore, for the dirty atmosphere, that the samples are taken from the same general atmospheric patch and that the roughness of the heterogeneous air mass, or the $\Delta\tau$, is small in comparison to the absolute value of τ.

The variability of τ with the number of points used in the Langley plot has been examined and repeated several times. It

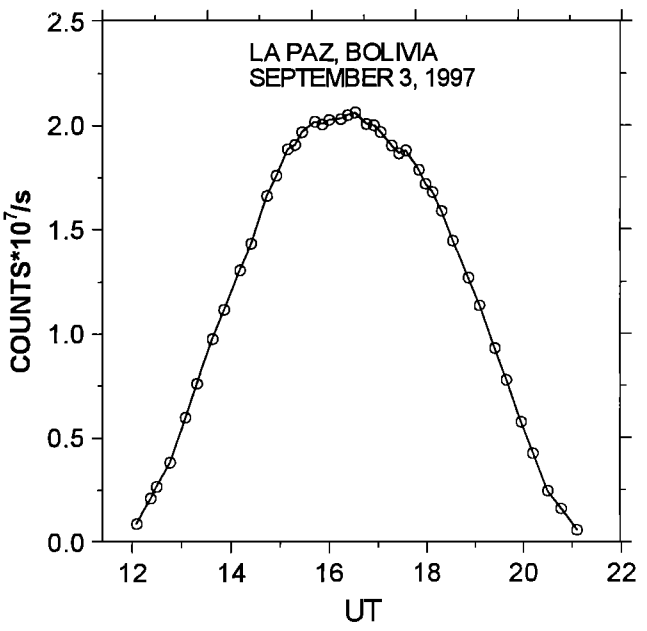

Figure 1. An example of direct solar radiation measured at 306.3 nm at La Paz, Bolivia, on September 3, 1997.

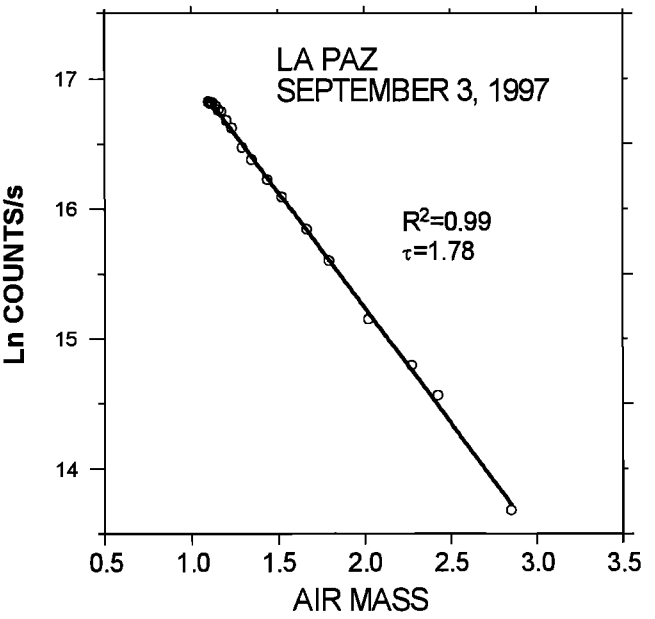

Figure 2. Typical Langley plot for data taken at La Paz, Bolivia, September 3, 1997, corresponding to data shown in Figure 1, morning data.

appears that the Langley method, can be used in, short time intervals on clear days, with only a few points (three to four) on the plot. On a day with a lot of aerosol mixed in the atmosphere, more points are recommended (at least six).

The results of the present measurements have been tested against observations made by other techniques. The deduced UV-B count rate at infinity, C_o, obtained from the Langley plot (as the intercept of the y axis), was one of the tested parameters. This variable can also be calculated using Beer's law, measured intensities, and τ (C_{oc}). The data points for 306.3 nm show some scatter, with a slope of 0.92 and a correlation coefficient r^2=0.65.

The ATLAS space shuttle missions were conducted in March 1992, April 1993, and November 1994, and included total and spectrally resolved solar irradiance [*Kaye and Miller*, 1996; *Cebula et al.*, 1996]. Comparing these data with the extrapolated Brewer data, there is again some scatter in the data; that is, the variability observed, for example, for La Paz has much larger variations than the satellite data. It is believed that such scatter of the Brewer data is the result of natural changes/variabilities that occur in the time interval necessary to build the Langley plot.

In addition to the satellite comparison, it is possible to compare (or extrapolate and compare) the optical depth information with the data obtained by *Ross et al.* [1997, 1998] during the Smoke, Clouds, and Radiation-Brazil (SCAR-B) field campaign of 1995, which took place in the cerrado region in Brazil [*Kaufman et al*, 1998; *King et al.*, 1998]. The Ross et al. data are obtained with a sunphotometer [*Holben et al.*, 1996], which measures the optical depth in the visible, up to near the UV-A region. The maximum values obtained by the sunphotometer and the values in the UV-B ranges (present work) seem to be at comparable levels; the minimum values of the UV-B data seem to be larger. However, this comparison must be interpreted with care since different conditions are involved.

2.3. Time Variations

The previous discussion has assumed that the air mass sampled was not entirely homogeneous (when smoke is present), but that

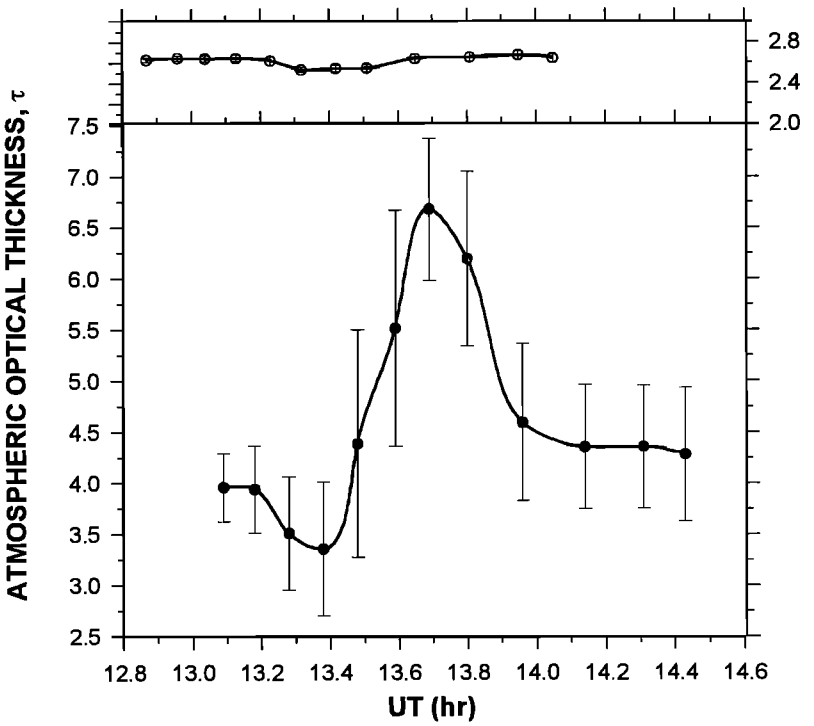

Figure 3. Example of optical thickness variation with time at the Campo Grande site, using six point running means of the UV-B observations: (top) clear day and (bottom) smoky day. Standard deviations are also shown.

its heterogeneity could be represented by a mean τ, where the predominant samples can be represented by an average background value, and a variability of $\Delta\tau$. This variability would be seen if the measurements could be made at very short time intervals. In practice, in order to show the time variability in τ, the results of about 1 hour (six complete sets of observations/samplings) have been used, and a typical variability found is shown in Figure 3 (for λ=306.3 nm). The time variation of the observations is expressed in this figure by obtaining τ from Langley plots of six sequential and independent data points (that is, six sequential direct Sun UV-B observation sets), but in the form of running means (that is, each Langley plot uses data points one to six, then two to seven, then three to eight, etc.). In this way a time variation in τ can be obtained that is of the same magnitude of the time interval between data points. The top panel shows the time variation obtained for a relatively clear day (Julian day 230), for which $\Delta\tau$ is very small (0.14) with standard errors of 0.05 (barely seen in the figure); the bottom panel shows the time variation for a day with strong biomass burning activity (Julian day 219), showing much larger $\Delta\tau$ variations (of the order of 3.3) with standard errors of about 1.15.

2.4. Morning-Afternoon Time Series of τ

Time series of τ variations are created by grouping the data set in half day periods (with about 20 data points each) for morning or afternoon average values. Results for the month of August 1999, at the three sites, for λ=306.3 nm, are plotted in Figure 4. For Campo Grande (bottom panel) the background value for τ is about 2.5, with maxima reaching about 4.5. While most of the data points have standard deviations of the order of $\pm$0.1, there are cases with values up to 5 times as large, associated with the passage of thicker air masses. The shape of the time variations is similar for the different wavelengths of Table 1. For λ=320.1 nm, shown in Figure 5, the background values are near 1.5, and the peaks reach maxima near 3.3.

The time series for the station La Paz is much smoother than the Campo Grande site, as expected. The results shown in Figure 4, for λ=306.3 nm, middle panel, show that the background value is near 2.0. Among the data points, two cases stand out, one for

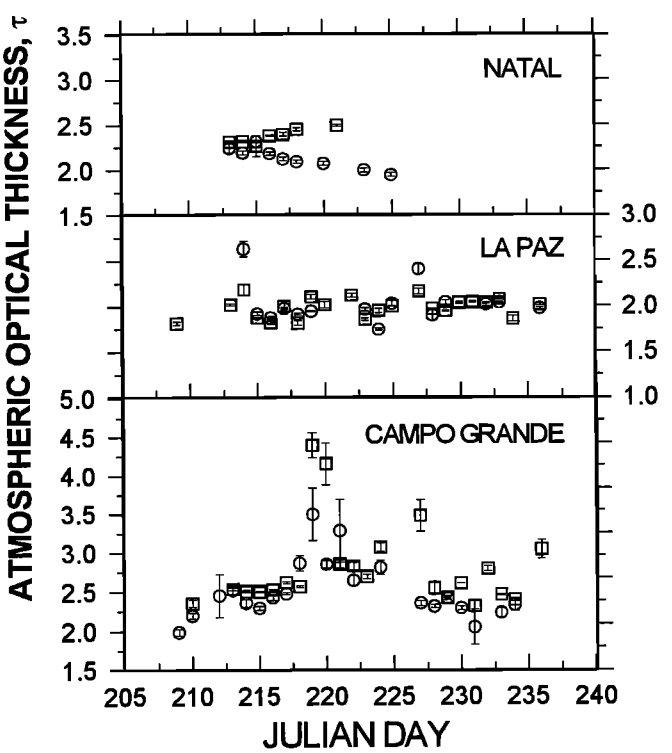

Figure 4. Time series of atmospheric optical thickness measurements τ at three sites for 306.3 nm. Morning (squares) and afternoon averages (circles) are shown for observations in August 1999.

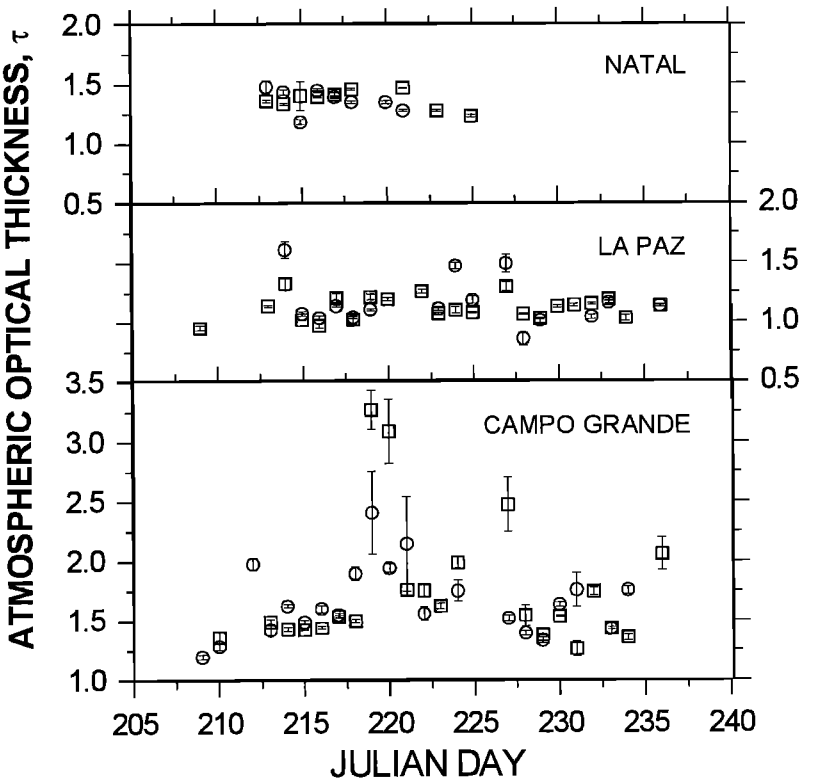

Figure 5. Time series of atmospheric optical thickness measurements τ at three sites for 320.1 nm. Morning (squares) and afternoon averages (circles) are shown for observations in August 1999.

day 214 (τ=2.6) and one for day 227 (τ=2.4). Note that the individual standard errors of the measurements are relatively small (±0.1) for all measurements at La Paz. The maximum time variability (Δτ) at this site is 1.0. For the longer wavelength (Figure 5), the predominant value is around 1.1, with maximum at about 1.6 and minimum at about 0.8.

At Natal, shown in the top panel of Figure 4, the results are similar in magnitude to the La Paz ones, with values between 1.8 and 2.5 (Δτ=0.7), with standard errors of the order of ±0.1. The results at the longer wavelength, 320.1 nm, shown in Figure 5 in the top panel, show a maximum at about 1.4 and minimum at 1.2. The shapes of the variations are similar to the shorter wavelength

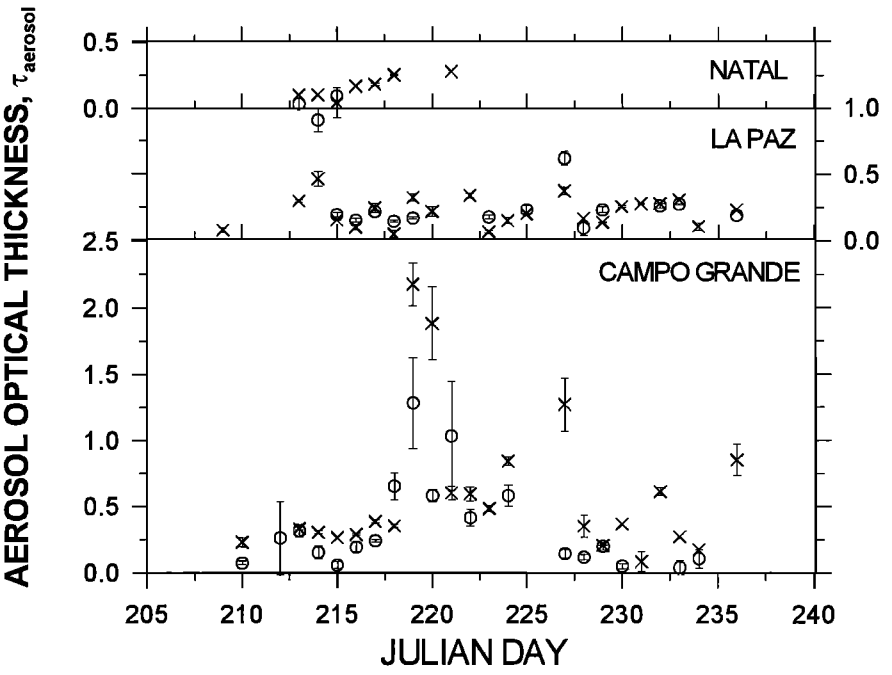

Figure 6. Time series of aerosol optical thickness measurements $\tau_{aerosol}$ at three sites for 306 3 nm. Morning (squares) and afternoon averages (circles) are shown for observations in August 1999.

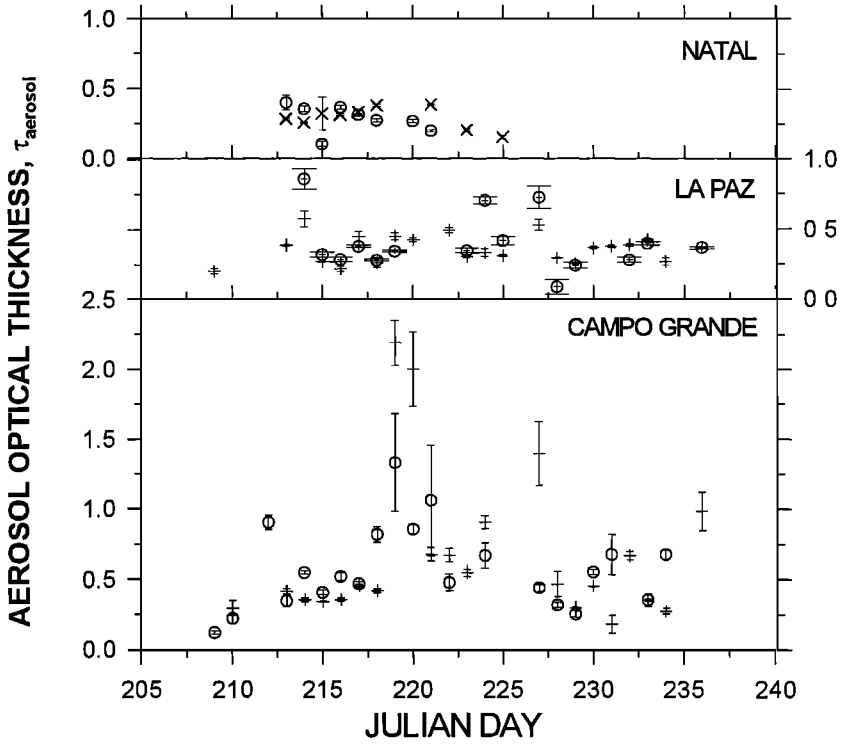

Figure 7. Time series of aerosol optical thickness measurements $\tau_{aerosol}$ at three sites for 320.1 nm. Morning (squares) and afternoon averages (circles) are shown for observations in August 1999.

(306.3 nm, Figure 4), but the absolute values are smaller, as expected.

The aerosol optical thickness $\tau_{aerosol}$ is considered next. Figure 6 shows the values deduced for Natal, La Paz, and Campo Grande for the same period of the previous figures. The aerosol optical thicknesses for Natal and La Paz have values from 0.0 to 0.25; at Campo Grande the background may be at slightly larger values, around 0.3, and perhaps with a secondary background of $\tau_{aerosol}$ around 0.6, and then sporadic large increases of up to 2.2, reflecting the presence of smoke from biomass burning. The same time sequence is shown in Figure 7 for the wavelength of 320.1 nm. Note that most of the larger variabilities shown in the τ data are the result of the variations seen in $\tau_{aerosol}$, as already mentioned, the ozone variation contribution being small and accounted for.

It is of interest to look at the individual contributions in τ, shown in Tables 3 and 4, for the two wavelength extremes. The contribution of SO_2 is always very small in this case; in a few cases, when the signal-to-noise ratio is small, the values are small

Table 3. Optical Thicknesses at 306.3 nm in the Morning Period for Campo Grande in August 1999

Day	τ	σ_τ	$\tau_{Rayleigh}$	τ_{ozone}	$\sigma_{\tau ozone}$	τ_{SO2}	$\sigma_{\tau SO2}$	$\tau_{aerosol}$	$\sigma_{\tau aerosol}$
209	-	-	1.06	1.14	0.08	-	-	-	-
210	2.36	0.05	1.06	1.06	0.03	0.04	0.10	0.19	-
212	-	-	1.06	1.13	0.01	0.02	0.01	-	-
213	2.54	0.01	1.06	1.15	0.01	0.01	0.01	0.33	0.01
214	2.51	0.01	1.06	1.14	0.01	0.01	0.01	0.30	0.01
215	2.5	0.00	1.06	1.17	0.01	0.01	0.01	0.26	-
216	2.53	0.01	1.06	1.18	0.01	0.01	0.01	0.28	-
217	2.62	0.01	1.06	1.17	0.01	0.01	0.01	0.37	-
218	2.57	0.01	1.06	1.15	0.00	0.01	0.01	0.34	0.00
219	4.39	0.16	1.06	1.15	0.01	0.04	0.01	2.14	0.16
220	4.16	0.27	1.06	1.21	0.01	0.01	0.01	1.88	0.27
221	2.85	0.05	1.06	1.19	0.01	0.01	0.01	0.60	0.05
222	2.83	0.05	1.06	1.17	0.01	0.01	0.01	0.59	0.05
223	2.69	0.03	1.06	1.15	0.01	0.00	0.02	0.48	0.01
224	3.07	0.05	1.06	1.17	0.04	-	-	0.84	0.03
227	3.48	0.20	1.06	1.15	0.01	-	-	1.27	0.20
228	2.54	0.08	1.06	1.13	0.01	-	-	0.35	0.08
229	2.42	0.01	1.06	1.15	0.01	0.00	0.01	0.21	-
230	2.60	0.00	1.06	1.17	0.01	0.00	0.01	0.37	-
231	2.31	0.07	1.06	1.16	0.01	0.01	0.01	0.08	0.07
232	2.8	0.03	1.06	1.12	0.01	0.01	0.01	0.61	0.02
233	2.46	0.01	1.06	1.13	0.02	-	-	0.27	-
234	2.4	0.02	1.06	1.16	0.04	-	-	0.18	-
236	3.04	0.12	1.06	1.13	0.01	0.01	0.01	0.85	0.12

Table 4. Optical Thicknesses at 320.1 nm in the Morning Period for Campo Grande in August 1999

Day	τ	σ_τ	$\tau_{Rayleigh}$	τ_{ozone}	$\sigma_{\tau ozone}$	τ_{SO2}	$\sigma_{\tau SO2}$	$\tau_{aerosol}$	$\sigma_{\tau aerosol}$
209	-	-	0.88	0.20	0.01	-	-	-	-
210	1.36	0.05	0.88	0.18	0.01	0.00	0.01	0.29	0.05
212	-	-	0.88	0.19	0.00	0.00	0.00	-	-
213	1.49	0.02	0.88	0.2	0.00	0.00	0.00	0.41	0.02
214	1.43	0.01	0.88	0.20	0.00	0.00	0.00	0.35	0.01
215	1.42	0.00	0.88	0.20	0.00	0.00	0.00	0.34	0.00
216	1.44	0.01	0.88	0.20	0.00	0.00	0.00	0.36	0.01
217	1.53	0.01	0.88	0.20	0.00	0.00	0.00	0.45	0.01
218	1.50	0.01	0.88	0.20	0.00	0.00	0.00	0.42	0.01
219	3.27	0.16	0.88	0.20	0.00	0.00	0.00	2.19	0.16
220	3.09	0.27	0.88	0.21	0.00	0.00	0.00	2.00	0.27
221	1.76	0.05	0.88	0.20	0.00	0.00	0.00	0.68	0.05
222	1.75	0.05	0.88	0.20	0.00	0.00	0.00	0.67	0.05
223	1.62	0.02	0.88	0.20	0.00	0.00	0.00	0.55	0.02
224	1.98	0.05	0.88	0.20	0.01	-	-	0.91	0.05
227	2.47	0.23	0.88	0.20	0.00	-	-	1.40	0.23
228	1.54	0.09	0.88	0.19	0.00	-	-	0.47	0.09
229	1.37	0.01	0.88	0.20	0.00	0.00	0.00	0.30	0.01
230	1.53	0.00	0.88	0.20	0.00	0.00	0.00	0.45	0.00
231	1.26	0.06	0.88	0.20	0.00	0.00	0.00	0.18	0.06
232	1.74	0.03	0.88	0.19	0.00	0.00	0.00	0.67	0.03
233	1.43	0.01	0.88	0.19	0.00	-	-	0.36	0.01
234	1.35	0.02	0.88	0.20	0.01	-	-	0.28	0.02
236	2.05	0.14	0.88	0.19	0.00	0.00	0.00	0.98	0.14

and negative. Note that although the aerosol component is the result of a subtraction of numbers of the same magnitude, the results are consistent with small standard deviations; that is, they are statistically significant. Tables 5-10 show the morning and afternoon averages of the aerosol optical thicknesses obtained and their standard deviations.

It is interesting to mention that there are a few cases in which larger wavelengths show larger optical thicknesses, which is contrary to the normal tendency of increasing values for lower wavelengths. It is possible that this is caused by observations of different air masses that have aerosol particles with different sizes, for example. It has been reported that the majority of the biomass burning aerosol particles seen in similar environments have a geometric mean particle diameter of about 0.1 μm, as observed with a differential mobility particle spectrometer [*Reid et al.*, 1996]. It is believed that the present measurements have been

Table 5. Numerical Values of Average Aerosol Optical Thickness $\tau_{aerosol}$ and Its Standard Deviation, for Campo Grande, MS, August 1999, for Five Wavelengths [a]

	306.3		310.1		313.5		316.8		320.1	
JD	$\tau_{aerosol}$	s.d.	$\tau_{aerosol}$	s.d.	$\tau_{aerosol}$	s.d.	$\tau_{aerosol}$	s.d.	$\tau_{aerosol}$	s.d.
210	0.23	0.03	0.34	0.04	0.28	0.05	0.29	0.05	0.30	0.05
213	0.33	0.01	0.43	0.02	0.39	0.02	0.41	0.02	0.42	0.02
214	0.31	0.01	0.36	0.01	0.33	0.01	0.35	0.01	0.36	0.01
215	0.27		0.40	0.01	0.33		0.34		0.34	
216	0.29	0.01	0.41	0.01	0.34	0.01	0.35	0.01	0.36	0.01
217	0.39	0.01	0.52	0.01	0.44	0.01	0.45	0.01	0.45	0.01
218	0.35	0.01	0.49	0.02	0.41	0.01	0.42	0.01	0.42	0.01
219	2.18	0.16	2.44	0.16	2.22	0.02	2.19	0.16	2.19	0.16
220	1.89	0.27	2.29	0.26	2.00	0.27	1.99	0.27	2.00	0.27
221	0.60	0.05	0.78	0.05	0.67	0.05	0.67	0.05	0.68	0.05
222	0.60	0.05	0.74	0.05	0.66	0.05	0.67	0.05	0.67	0.05
223	0.49	0.02	0.63	0.03	0.54	0.03	0.54	0.03	0.55	0.02
224	0.85	0.03	1.02	0.05	0.9	0.05	0.91	0.05	0.91	0.05
227	1.27	0.20	1.34	0.21	1.34	0.22	1.38	0.22	1.40	0.23
228	0.35	0.08	0.59	0.08	0.44	0.09	0.46	0.09	0.47	0.09
229	0.21		0.35		0.27	0.01	0.29	0.01	0.3	0.01
230	0.37		0.50		0.43		0.45		0.45	
231	0.09	0.07	0.18	0.07	0.14	0.07	0.17	0.07	0.18	0.06
232	0.62	0.03	0.74	0.04	0.66	0.03	0.67	0.03	0.67	0.03
233	0.27		0.18		0.30		0.35	0.01	0.36	0.01
234	0.18		0.32	0.01	0.25	0.02	0.27	0.02	0.28	0.02
236	0.85	0.12	1.01	0.12	0.93	0.13	0.96	0.13	0.98	0.14

[a] Morning values; s.d. refers to the standard deviation.

Table 6. Numerical Values of Average Aerosol Optical Thickness $\tau_{aerosol}$, and Its Standard Deviation, for Campo Grande, MS, August 1999, for Five Wavelengths [a]

	306.3		310.1		313.5		316.8		320.1	
JD	$\tau_{aerosol}$	s.d.	$\tau_{aerosol}$	s.d.	$\tau_{aerosol}$	s.d.	$\tau_{aerosol}$	s.d.	$\tau_{aerosol}$	s.d.
209			0.07		0.08		0.12		0.12	0.01
210	0.08	0.02	0.24	0.03	0.21	0.03	0.22	0.03	0.22	0.03
212	0.26	0.28	0.75	0.09	0.78	0.08	0.87	0.04	0.9	0.05
213	0.32	0.05	0.36	0.05	0.33	0.04	0.35	0.04	0.35	0.04
214	0.16	0.05	0.48	0.02	0.52	0.01	0.55	0.01	0.55	0.01
215	0.06	0.02	0.39	0.01	0.38	0.02	0.41	0.02	0.41	0.02
216	0.19	0.03	0.48	0.03	0.49	0.03	0.52	0.03	0.52	0.03
217	0.24	0.01	0.47	0.02	0.44	0.02	0.47	0.02	0.47	0.02
218	0.66	0.10	0.83	0.09	0.84	0.09	0.87	0.09	0.82	0.06
219	1.28	0.34	1.37	0.34	1.32	0.35	1.33	0.35	1.33	0.35
220	0.59	0.05	0.74	0.04	0.79	0.03	0.84	0.03	0.86	0.03
221	1.03	0.41	1.10	0.41	1.06	0.40	1.06	0.40	1.06	0.40
222	0.42	0.06	0.45	0.06	0.45	0.06	0.47	0.06	0.48	0.06
224	0.59	0.08	0.68	0.09	0.64	0.09	0.67	0.09	0.67	0.09
227	0.15	0.03	0.41	0.02	0.41	0.02	0.44	0.02	0.44	0.02
228	0.12	0.02	0.30	0.02	0.29	0.02	0.32	0.02	0.32	0.02
229	0.20	0.03	0.25	0.03	0.23	0.02	0.25	0.02	0.25	0.02
230	0.05	0.02	0.54	0.02	0.52	0.02	0.55	0.02	0.55	0.02
231			0.75	0.14	0.64	0.14	0.67	0.14	0.68	0.14
233	0.04	0.05	0.34	0.04	0.32	0.05	0.35	0.05	0.36	0.05
234	0.11	0.07	0.64	0.05	0.65	0.05	0.71	0.05	0.68	0.03

[a] Afternoon values.

Table 7. Numerical Values of Average Aerosol Optical Thickness $\tau_{aerosol}$, and Its Standard Deviation, for La Paz, 1999, for Five Wavelengths [a]

	306.3		310.1		313.5		316.8		320.1	
JD	$\tau_{aerosol}$	s.d.	$\tau_{aerosol}$	s.d.	$\tau_{aerosol}$	s.d.	$\tau_{aerosol}$	s.d.	$\tau_{aerosol}$	s.d.
209	0.08	0.02	0.68	0.02	0.62	0.02	0.52	0.02	0.20	0.02
213	0.30	0.01	0.59	0.01	0.56	0.01	0.53	0.01	0.38	0.01
214	0.46	0.05	0.93	0.05	0.89	0.05	0.82	0.05	0.57	0.06
215	0.15	0.00	0.71	0.02	0.65	0.02	0.56	0.02	0.26	0.00
216	0.10	0.02	0.61	0.03	0.57	0.03	0.49	0.02	0.22	0.02
217	0.24	0.03	1.15	0.06	1.09	0.06	0.97	0.06	0.44	0.04
218	0.05	0.03	1.12	0.06	1.05	0.06	0.90	0.06	0.26	0.03
219	0.32	0.03	0.85	0.03	0.81	0.03	0.73	0.03	0.45	0.02
220	0.22	0.04	1.05	0.05	0.99	0.04	0.88	0.03	0.42	0.01
222	0.34	0.02	1.22	0.03	1.15	0.02	1.01	0.02	0.49	0.02
223	0.06	0.01	0.79	0.03	0.76	0.02	0.68	0.02	0.30	0.01
224	0.15	0.02	0.99	0.05	0.93	0.04	0.81	0.04	0.33	0.03
225	0.20		0.65	0.04	0.61	0.03	0.55	0.03	0.31	0.01
227	0.37	0.03	1.11	0.11	1.07	0.10	0.96	0.09	0.53	0.04
228	0.17		0.68	0.03	0.64	0.03	0.57	0.02	0.29	0.01
229	0.14	0.00	0.62	0.02	0.57	0.02	0.51	0.01	0.25	0.01
230	0.26	0.01							0.36	0.01
231	0.28	0.01	0.74	0.02	0.69	0.02	0.63	0.02	0.38	0.01
232	0.28		0.75	0.03	0.70	0.03	0.64	0.03	0.39	0.01
233	0.31		0.76	0.03	0.72	0.03	0.66	0.02	0.42	0.01
234	0.11	0.03	0.88	0.04	0.82	0.04	0.72	0.03	0.27	0.03
236	0.23		0.71	0.02	0.67	0.02	0.61	0.01	0.37	0.01

[a] Morning values.

Table 8. Numerical Values of Average Aerosol Optical Thickness $\tau_{aerosol}$, and Its Standard Deviation, for La Paz, 1999, for Five Wavelengths [a]

	306.3		310.1		313.5		316.8		320.1	
JD	$\tau_{aerosol}$	s.d.	$\tau_{aerosol}$	s.d.	$\tau_{aerosol}$	s.d.	$\tau_{aerosol}$	s.d.	$\tau_{aerosol}$	s.d.
214	0.91	0.09	0.78	0.09	0.75	0.09	0.78	0.08	0.86	0.07
215	0.19	0.02	0.34	0.02	0.32	0.02	0.33	0.02	0.32	0.02
216	0.15	0.01	0.32	0.02	0.30	0.02	0.31	0.02	0.28	0.02
217	0.22	0.01	0.41	0.01	0.39	0.01	0.40	0.01	0.37	0.01
218	0.14	0.01	0.32	0.01	0.29	0.01	0.30	0.01	0.28	0.01
219	0.17	0.01	0.37	0.01	0.35	0.01	0.36	0.01	0.34	0.01
223	0.18	0.02	0.38	0.02	0.36	0.02	0.37	0.02	0.34	0.02
224	0.54		0.01	0.67	0.02	0.67	0.01	0.70	0.03	
225	0.23	0.03	0.45	0.03	0.43	0.03	0.44	0.03	0.41	0.03
227	0.62	0.05	0.66	0.06	0.66	0.07	0.70	0.08	0.72	0.08
228	0.09	0.06	0.11	0.05	0.08	0.05	0.09	0.05	0.09	0.05
229	0.23	0.02	0.27	0.02	0.24	0.02	0.25	0.02	0.24	0.02
230	0.74		0.02	0.69	0.02	0.62	0.02			
232	0.26	0.02	0.33	0.03	0.30	0.03	0.30	0.03	0.28	0.02
233	0.27	0.01	0.43	0.01	0.41	0.01	0.42	0.01	0.40	0.01
236	0.19		0.40	0.01	0.38	0.01	0.40	0.01	0.37	0.01

[a] Afternoon values.

Table 9. Numerical Values of Average Aerosol Optical Thickness $\tau_{aerosol}$ and Its Standard Deviation, for Natal, 1999, for Five Wavelengths [a]

	306.3		310.1		313.5		316.8		320.1	
213	0.10		0.31		0.29		0.30	0.01	0.28	0.01
214	0.10		0.29		0.26		0.27	0.01	0.26	0.01
215	0.04	0.11	0.34	0.12	0.33	0.12	0.34	0.12	0.32	0.12
216	0.17		0.35	0.01	0.33	0.01	0.33	0.01	0.31	0.01
217	0.18	0.01	0.37	0.02	0.35	0.02	0.35	0.02	0.33	0.02
218	0.25	0.00	0.43	0.01	0.40	0.01	0.40	0.01	0.38	0.01
221	0.28		0.44		0.41	0.00	0.40	0.00	0.39	0.00

[a] Morning values.

Table 10. Numerical Values of Average Aerosol Optical Thickness $\tau_{aerosol}$, and Its Standard Deviation, for Natal, 1999, for Five Wavelengths [a]

	306.3		310.1		313.5		316.8		320.1	
JD	$\tau_{aerosol}$	s.d.	$\tau_{aerosol}$	s.d.	$\tau_{aerosol}$	s.d.	$\tau_{aerosol}$	s.d.	$\tau_{aerosol}$	s.d.
213	0.03	0.04	0.41	0.05	0.39	0.03	0.42	0.05	0.40	0.05
214		0.37	0.01	0.36	0.02	0.37	0.02	0.36	0.02	
215	0.09		0.16	0.01	0.12	0.02	0.12	0.02	0.10	0.02
216		0.36	0.01	0.36	0.01	0.37	0.01	0.37	0.01	
217		0.31		0.31	0.01	0.32	0.01	0.31	0.01	
218		0.26		0.26	0.01	0.28	0.01	0.27	0.01	
220		0.24		0.25	0.01	0.27	0.01	0.27	0.01	
221								0.20	0.01	
223		0.17		0.18		0.20	0.00	0.20	0.01	
225		0.10	0.00	0.12	0.01	0.15	0.01	0.15	0.01	

[a] Afternoon values.

made under conditions where such particles were also present. *Remer et al.* [1998] point out that the optical properties in the biomass burning regime are dominated by small particles, but in addition, as noted by *Kaufman et al.* [1998], smoke particles emitted by fires may increase their radius by as much as 60% during their first 3 days in the atmosphere by condensation and coagulation.

3. Conclusions

Three Brewer spectrophotometers have been operated simultaneously at three sites during the month of August 1999, in order to compare the atmospheric total optical thickness, and the aerosol optical thickness, in the UV-B spectral range. One of these sites, Campo Grande, was set up in the biomass burning region of

central Brazil, in order to evaluate the absolute size and time variations of the total optical thickness using the Langley method. Since the spectrophotometer also measures ozone, the major absorber in the UV-B spectral range, and SO_2, and since the Rayleigh contribution can be readily calculated, it was also possible to deduce the aerosol optical thickness. Major conclusions are as follows:

1. The Langley method, which has been used extensively for obtaining the optical thickness in the visible spectral ranges, has been successfully applied also to the UV-B range; the method can be used for τ (the total atmospheric optical thickness), $\tau_{aerosol}$ (the aerosol optical thickness), and I_o (the extraterrestrial component of UV-B intensity.

2. The absolute values of optical thicknesses have been determined in the UV-B spectral range from regions of relatively clean air to a region of considerable biomass burning activity. Absolute values for τ at Natal and La Paz were near 2.0 and at Campo Grande, between 2.5 and 3.0, but with occasional highs of about 4.5. For $\tau_{aerosol}$, Natal and La Paz had values between 0.0 and 0.4, whereas Campo Grande had most values near 0.4, with occasional highs near 1.0, 1.2, and 2.2.

Acknowledgments. We are grateful to Jose Roberto Chagas for the field work at EMPAER, in Campo Grande, MS, during the month of August 1999. Financial support from INPE (basic infrastructure), EMPAER (infrastructure in CG), CAPES (scholarship for A.A.S.), and FAPESP (several grants) is acknowledged. The international calibration of the Brewer spectrophotometers has been made by Ken Lamb.

References

Brewer, A.W., A replacement for the Dobson spectrophotometer?, *Pure Appl. Geophys., 106-108*, 919-927, 1973.

Cebula, R.P., G.O. Thuillier, M.E. Vanhoosier, E. Hilsenrath, M. Herse, G.E. Brueckner, and P.C. Simon, Observations of the solar irradiance in the 200-350 nm interval during the ATLAS-1 mission; A comparison among three sets of measurements - SSBUV, SOLSPEC, and SUSIM, *Geophys. Res. Lett., 23*, 2289-2292, 1996.

Fioletov, V.E., E. Briffioen, J.B. Kerr, and D.I. Wardle, Influence of volcanic sulfur dioxide on spectral UV irradiance as measured by Brewer spectrophotometers, *Geophys. Res. Lett., 25*, 1665-1668, 1998.

Frederick, J., and D. Lubin, The budget of biologically active ultraviolet radiation in the Earth-atmosphere system, *J. Geophys. Res., 93*, 3825-3832, 1988.

Froehlich, C.G., and E. Shaw, New determination of Rayleigh scattering in the terrestrial atmosphere, *App. Opt., 19*, 1773-1775, 1980.

Holben, B.N., A. Setzer, T.F. Eck, A. Pereira and I. Slutsker, Effect of dry-season biomass burning on Amazon basin aerosol concentrations and optical properties, 1992-1994, *J. Geophys. Res., 101*, 19,465-19,481, 1996.

Kaufman, Y.J., et al., Smoke, Cloud and Radiation-Brazil (SCAR B) experiment, *J. Geophys. Res., 103*, 31,783-31,808, 1998.

Kaye, J.A. and T.L. Miller, The ATLAS series of shuttle missions, *Geophys. Res. Lett., 23*, n 17, p 2285-2288, 1996.

King, M.D., S.-C. Tsay, S.A. Ackerman, and N.F. Larsen, Discriminating heavy aerosol, clouds, and fires during SCAR-B: Application of airborne multispectral MAS data, *J. Geophys. Res., 103*, 31,989-31,999, 1998.

Kirchhoff, V. W.J.H., Increasing concentrations of CO and O_3 - Rising deforestation rates and increasing tropospheric carbon monoxide and ozone in Amazonia, *Environ. Sci. Pollut. Res., 3*, 210-212, 1996.

Kirchhoff, V.W.J.H., F. Zamorano, and C.A.R. Casiccia, UV-B enhancements at Punta Arenas, Chile, *J. Photochem. Photobiol.*, Part *B: Biology, 38*, 174-177, 1997a.

Kirchhoff, V.W.J.H., C.A.R. Casiccia, and F. Zamorano, The ozone hole over Punta Arenas, Chile, *J. Geophys. Res., 102*, 8945-8953, 1997b.

Kirchhoff, V.W.J.H., Y. Sahai, C.A.R. Casiccia, F. Zamorano, and V. Valderrama, Observations of the 1995 ozone hole over Punta Arenas, Chile, *J. Geophys. Res., 102*, 16,109-16,120, 1997c.

Krishnamurti, T.N., B. Jha, J. Prospero, A. Jayaraman, and V. Ramanathan, Aerosol and pollutant transport and their impact on radiative forcing over the tropical Indian Ocean during the January-February 1996 pre-INDOEX cruise, *Tellus, Ser. B, 50*, 521-542, 1998.

Kylling, A., F. Bais, M. Blumthaler, J. Schreder, C.S. Zerefos, and E. Kosmidis, Effect of aerosol on solar UV irradiances during the photochemical activity and solar ultraviolet radiation campaign, *J. Geophys. Res., 103*, 26,051-26,060, 1998.

Logan, J.A. and V.W.J.H. Kirchhoff, Seasonal variations of tropospheric ozone at Natal, Brazil. *J. Geophys. Res., 91*, 7875-7881, 1986.

Longo, K.M., A.M. Thompson, V.W.J.H. Kirchhoff, L.A. Remer, S.R. de Freitas, M.A.F. Silva Dias, P. Artaxo, W. Hart, J.D. Spinhirne, and M. Yamasoe, Correlation between smoke and tropospheric ozone concentrations in Cuiabá during smoke, clouds, and radiation-Brazil (SCAR-B), *J. Geophys. Res., 104*, 12,113-12,129, 1999.

Olson, J.R., J. Fishman, V.W.J.H. Kirchhoff, D. Nganga, and B. Cros, An analysis of the distribution of O3 over the southern Atlantic region, *J. Geophys. Res., 101*, 24,083-24,093, 1996.

Qiu, J., A method to determine atmospheric aerosol optical depth using total direct radiation, *J. Atmos. Sci., 55*, 744-757, 1998.

Reid, J.S., P.V. Hobbs, and R.J. Ferek, Physical and Chemical characteristics of biomass burning aerosols in Brazil, *in* SCAR-B proceedings, edited by V.W.J.H. Kirchhoff, Transtec Ed., pp. 165-169, São José dos Campos, 1996.

Remer, L.A., Y.J. Kaufman, B.N. Holben, A.M. Thompson, and D. McNamara, Biomass burning aerosol size distribution and modeled optical properties, *J. Geophys. Res., 103*, 31,879-31,891, 1998.

Ross, J.L., P.V. Hobbs, and B. Holben, Direct radiative closure experiments on smoke from biomass burning in Brazil, in SCAR B proceedings, edited by V.W.J.H. Kirchhoff, pp. 177-182, Transtec Ed., São José dos Campos, 1997.

Ross, J.L., P.V. Hobbs, and B. Holben, Radiative characteristics of regional hazes dominated by smoke from biomass burning in Brazil: closure tests and direct radiative forcing, *J. Geophys. Res., 103*, 31,925-31,941, 1998.

Sahai, Y., V.W.J.H. Kirchhoff, , and P.C. Alvala, Pinatubo eruptions: effects on stratospheric O_3 and SO_2 over Brazil, *J. Atmos. Terr. Phys., 59*, 265-269, 1997.

Teillet, F.M., Rayleigh optical depth comparisons from various sources, *Appl.Opt., 29*, 1897-1900, 1990.

Wenny, B.N., J.S. Schafer, J.J. DeLuisi, V.K. Saxena, W.F. Farnard, I.V. Petropavloviskh, and A.J. Vergamini, A study of regional aerosol radiative properties and effects on ultraviolet-B radiation, *J. Geophys. Res., 103*, 17,083-17,097, 1998.

C.A. Costa, Empresa de Pesquisa, Assistência Técnica e Extensão Rural. Campo Grande, Brazil.(cesarc@empaer. pantanal.br)

V.W.J.H. Kirchhoff and N.P. Leme, Instituto Nacional de Pesquisas Espaciais, 12201-970 São José dos Campos, São Paulo, Brazil. (kir@dir.inpe.br; nleme@dge.inpe.br)

H.G. Pavão, Fundação Universidade Federal de Mato Grosso do Sul, Campo Grande, Brazil (hpavao@nin.ufms.br)

A.A. Silva, Pontifícia Universidade Católica de Minas Gerais, Belo Horizonte, Minas Gerais (abel@dge.inpe.br)

F. Zaratti, Universidad Mayor de San Andres, La Paz, Bolívia (ozono@mail.ma.magalink.com)

(Received April 3, 2000; revised August 9, 2000;
accepted August 9, 2000.)